

*ICANS-XI International Collaboration on Advanced Neutron Sources
KEK, Tsukuba, October 22-26, 1990*

Photons and Neutrons

Gen Shirane
Brookhaven National Laboratory
Upton, New York 11973

A review is given of two selected topics in current activities of synchrotron x-ray studies; magnetic x-ray scattering and inelastic x-ray scattering. These are the research areas where photons and neutrons directly compete and supplement each other.

I. MAGNETIC X-RAY SCATTERING

A great deal of progress has been made in the field of magnetic x-ray scattering with synchrotron radiation. A series of high resolution studies on Ho and other rare earth magnetic structures has revealed many important features of spin arrangements, which escaped clarification by previous neutron diffraction studies. One such example is shown in Fig. 1, taken from the study of the spiral structure in Ho by Gibbs et al.⁽¹⁾. They discovered that the incommensurate periodicity of Ho below $T_N=131\text{K}$ is not continuous and locks in specific rational fractions such as $2/11$ and $5/27$. These ratios can be naturally explained by spin-slip models. For example, the $\tau_m=5/27$ structure is constructed by one spin slip for every 9 atomic layers; namely 4 pairs of spins followed by 1 single spin as depicted on the right side of Fig. 1.

This spin slip creates the interplanar lattice modulation caused by the magnetic-elastic interaction. This periodicity is $2/9$, which is different from the magnetic period $5/27$. These two peaks, one magnetic and the other charge, are clearly seen in Fig. 1 and they have different line widths. These figures are a clear demonstration of the power of the high intensity and resolution offered by synchrotron x-ray sources.

Magnetic x-ray scattering recently entered into its next stage of development when the resonance at the absorption edge⁽²⁻⁴⁾ was shown to enhance the Ho magnetic cross section by a factor of 50. Fig. 2 shows the effect of the L_{III} absorption edge at 8.07KeV , on the $\text{Ho}(002)^+$ magnetic peak. This intensity enhancement of course gives a better visibility for the magnetic peak, which is usually much weaker than the charge peak at x-ray energies outside of the resonance region. Very recently, the resonant magnetic scattering was studied⁽⁵⁾ in antiferromagnetic UO_2 ; the enhancement factor here is 10^6 !

One essential difference between magnetic x-ray scattering and its neutron counterpart concerns the contribution of the orbital moment. For neutrons, all magnetic scattering

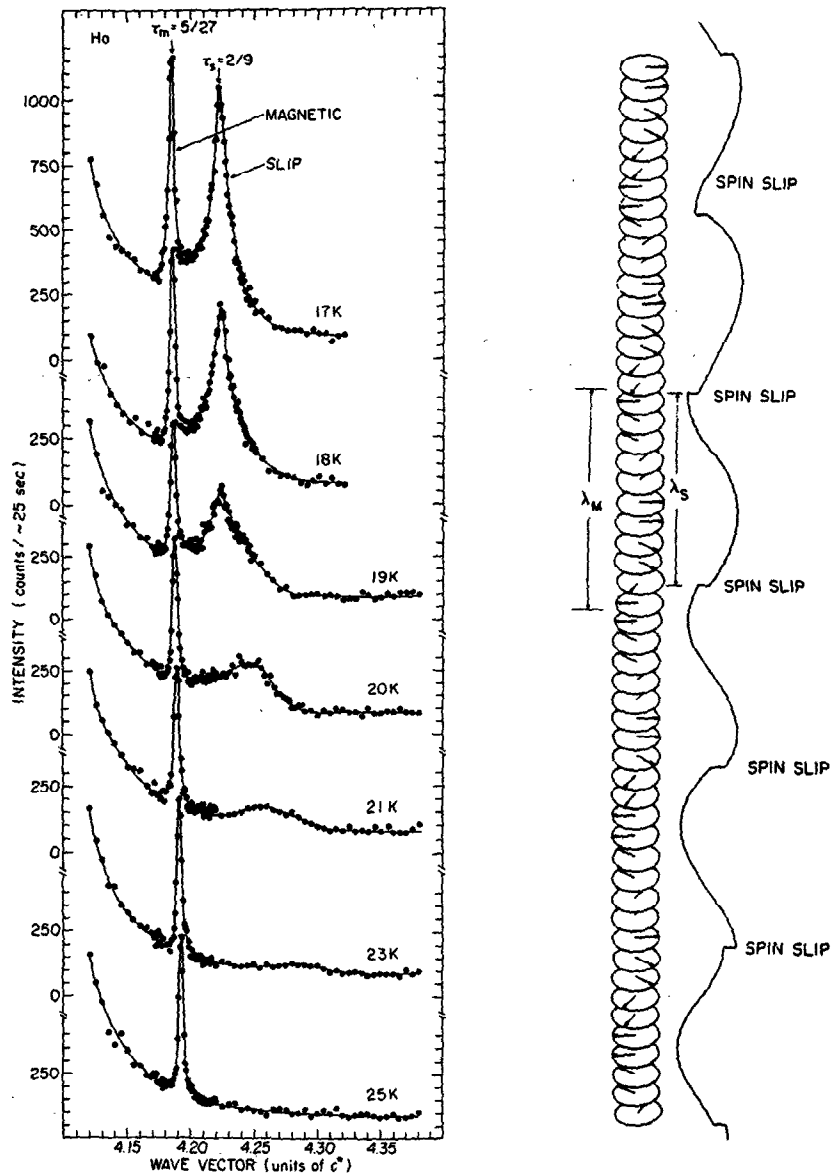


Fig. 1 Synchrotron x-ray diffraction pattern of the satellite above the (004) Bragg peak. The scattering pattern reflects both magnetic (5/27) and charge (2/9) modulations depicted on the spin slip model. After Gibbs et al. (Ref. 1)

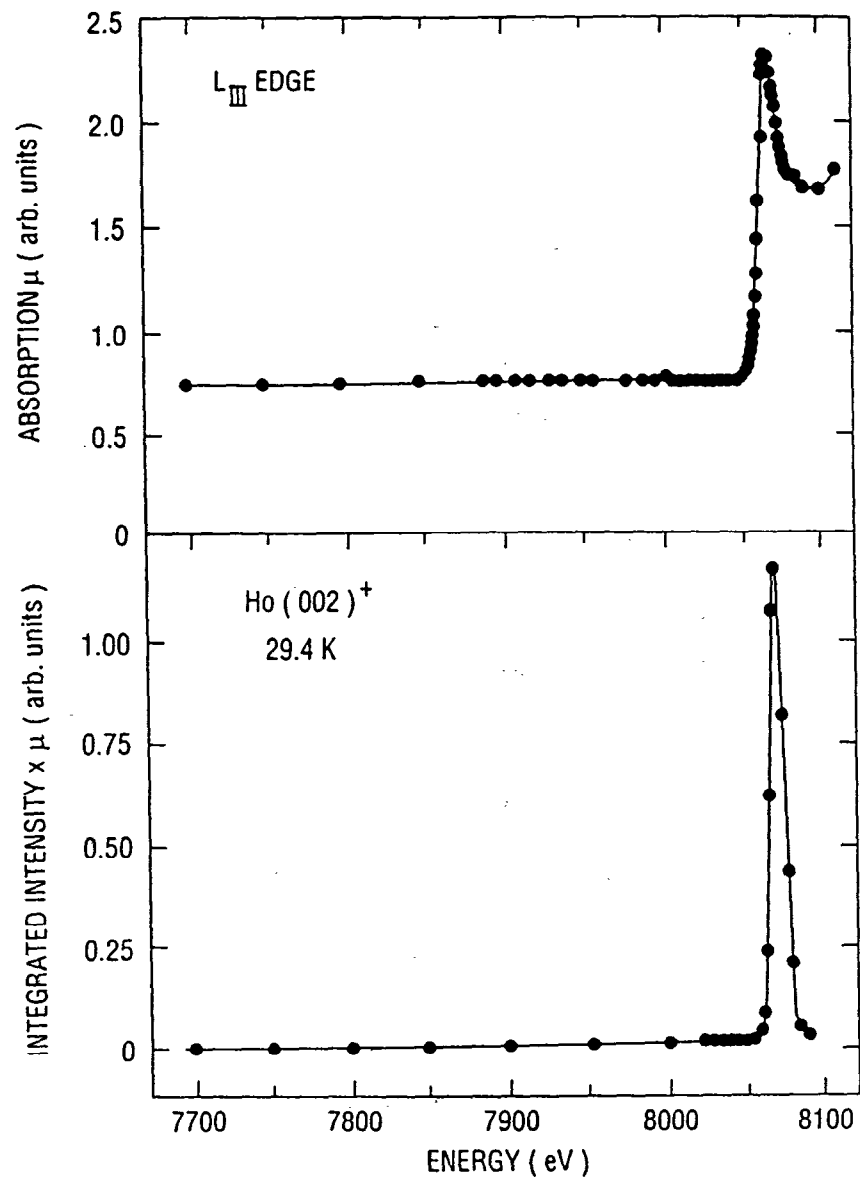


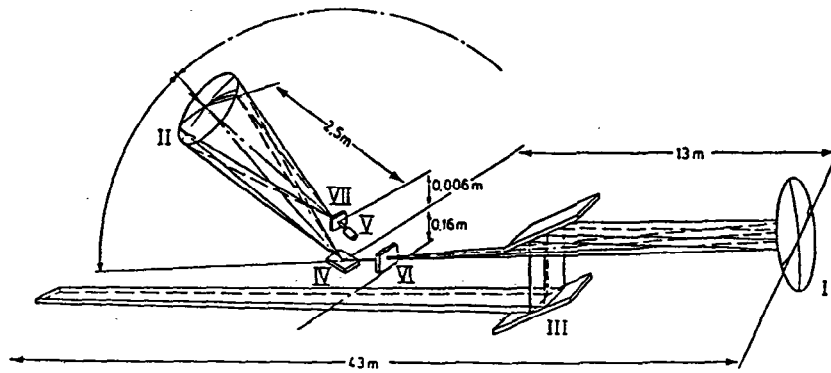
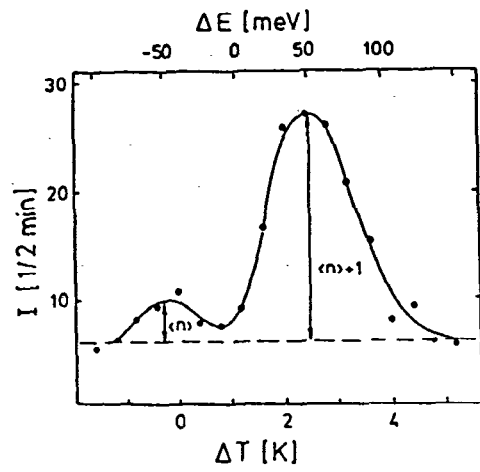
Fig. 2 Top: The absorption measured from a thin film. Bottom: The integrated magnetic intensity of the (002)⁺ reflection of Ho near the L_{III} edge. After Gibbs et al. Ref. (4).

(spin and orbital) is governed by the magnetic interaction vector \vec{q} , the projection of the magnetic moment on the plane perpendicular to the scattering vector \mathbf{Q} . Thus, the orbital moment reveals itself only by having a different form factor from that of spin. In the x-ray case, the σ and π polarizations of the scattered beam have different contributions from spin and orbital parts. Thus it is possible to separate out the two components using a polarization analyzer. This technical aspect is described in detail in a comprehensive paper by Gibbs et al⁽⁴⁾ on Ho magnetic scattering. Thus, by combining both neutron and x-ray data, one may be able to get definitive information on both components of the magnetization.

II. INELASTIC X-RAY SCATTERING

The second area where x-ray scattering is beginning to overlap with neutron research is direct inelastic x-ray scattering. Because of its favorable energy-wavelength relation, neutron scattering has been the natural tool for the direct observation of elementary excitations in condensed matter. The most commonly used neutrons have 14 meV of energy and a 2.3Å in wavelength. The energy of x-rays with the same wavelength is 5 KeV. In order to attain a sufficient energy resolution for phonon studies, one has to use backscattering from a perfect crystal. This type of experimental arrangement became feasible recently because of the brightness of x-rays emitted by synchrotron and storage rings. A successful test experiment was already reported by Burkel et al^(6,7) and is shown in Fig. 3. The monochromator I and analyzer II both consist of spherically bent silicon disks, grooved crosswise to reduce strains, and operate under extreme Bragg back reflection (777) with $\theta = 89.96$ at the monochromator and $\theta = 89.86$ at the analyzer. The beam is directed from the premonochromator III into the monochromator I and finally focused on the sample IV. The insert in Fig. 3 shows an example of phonon scans of diamond at (4,2,0,0). $\langle n \rangle$ is the Bose occupation factor. The scan clearly demonstrates the imbalance between energy gain and loss. The energy scan was carried out by varying the temperature of the analyzer crystal. A change of 1° corresponds to an energy change of 30 meV. An energy resolution of 17meV was obtained at the setup located at the hard x-ray wiggler line W2 at HASYLAB.

A similar inelastic x-ray scattering project was initiated at Brookhaven in 1980. A special crystal bender was constructed and tested by Fujii et al⁽⁸⁾ using an ungrooved crystal. 12.9 KeV x-rays from a white beam (20 x 2.5 mm²) were diffracted at $\theta = 89^\circ$ by the Si (880) reflection. The best focusing position gave the smallest spot (0.2 x 0.08 mm²) and this focused spot is more than three order of magnitude brighter than the unfocused beam. This project has recently been reactivated and a systematic effort is now underway to construct a larger beam bender for a Si crystal 125 mm in diameter. This analyzer crystal must be grooved and a procedure has been developed to dice the Si (111) surface into 0.2 x 0.2 mm blocks, 0.7 mm in height, separated by 0.05 mm wide channels⁽⁹⁾.



- | | | |
|-----------------|----------------------|--------------|
| I monochromator | III premonochromator | V detector |
| II analyser | IV sample | VI VII slits |

Fig. 3 Schematic setup of the instrument "INELAX" by Burkel et al (Ref 7).

It has already been demonstrated (6,7) that a direct observation of phonon excitations can be made using a back scattering x-ray arrangement and, as examples, the Be and diamond dispersion curves have been mapped out and show good agreement with neutron scattering data. The next step is the study of electronic excitations, the unique capability of the x-ray setup. With three large 7 GeV x-ray rings now under construction around the world, significant intensity gains are expected for this type of x-ray scattering in the near future.

I would like to thank Y. Fujii, P. M. Gehring, D. Gibbs, J. B. Hastings, G. H. Lander, D. E. Moncton, and D. P. Siddons for stimulating discussions. Work at Brookhaven was supported by the Division of Materials Sciences, U.S. Department of Energy under contract No. DE-AC02-76CH00016.

References

1. D. Gibbs, D. E. Moncton, K. L. D'Amico, J. Bohr, and B. H. Grier, *Phys. Rev. Lett* **55**, 234 (1985).
2. D. Gibbs, D. R. Harshman, E. D. Isaacs, D. B. McWhan, D. Mills, and C. Vettier, *Phys. Rev. Lett* **61**, 1241 (1988).
3. J. P. Hannon, G. T. Trammell, M. Blume, and D. Gibbs, *Phys. Rev. Lett* **61**, 1241 (1988).
4. D. Gibbs, G. Grübel, D. R. Harshman, E. D. Isaacs, D. B. McWhan, D. Mills, and C. Vettier, *Phys. Rev. B*, to be published.
5. G. H. Lander and D. Gibbs, Private Communications.
6. B. Dorner, E. Burkel, Th. Illini, and J. Peisl, *Z. Phys. B. Condensed Matter* **69**, 179 (1987).
7. E. Burkel, B. Dorner, Th. Illini and J. Peisl, *Rev. Sci. Instrum.* **60**, 1671 (1989).
8. Y. Fujii, J. B. Hastings, S. L. Ulc and D. E. Moncton. Report at SSRL Users Group Meeting, 1981, unpublished.
9. P. M. Gehring, J. M. Tranquada, D. P. Siddons, Private Communications.